

A Wide Dynamic Range NUC Algorithm for IRCS Systems

Li-Hua CAI, Feng-Yun HE and Song-Tao CHANG

*Changchun Institute of Optics, Fine Mechanics and Physics,
Chinese Academy of Sciences, Changchun 130033, China*

Zhou LI*

*Changchun Institute of Optics, Fine Mechanics and Physics,
Chinese Academy of Sciences, Changchun 130033, China and
University of Chinese Academy of Sciences, Beijing 100049, China*

(Received 4 May 2018, in final form 16 July 2018)

Uniformity is a key feature of state-of-the-art infrared focal planed array (IRFPA) and infrared imaging system. Unlike traditional infrared telescope facility, a ground-based infrared radiant characteristics measurement system with an IRFPA not only provides a series of high signal-to-noise ratio (SNR) infrared image but also ensures the validity of radiant measurement data. Normally, a long integration time tends to produce a high SNR infrared image for infrared radiant characteristics radiometry system. In view of the variability of and uncertainty in the measured target's energy, the operation of switching the integration time and attenuators usually guarantees the quality of the infrared radiation measurement data obtained during the infrared radiant characteristics radiometry process. Non-uniformity correction (NUC) coefficients in a given integration time are often applied to a specified integration time. If the integration time is switched, the SNR for the infrared imaging will degenerate rapidly. Considering the effect of the SNR for the infrared image and the infrared radiant characteristics radiometry above, we propose a-wide-dynamic-range NUC algorithm. In addition, this essay derives and establishes the mathematical modal of the algorithm in detail. Then, we conduct verification experiments by using a ground-based MWIR(Mid-wave Infared) radiant characteristics radiometry system with an $\varnothing 400$ mm aperture. The experimental results obtained using the proposed algorithm and the traditional algorithm for different integration time are compared. The statistical data shows that the average non-uniformity for the proposed algorithm decreased from 0.77% to 0.21% at 2.5 ms and from 1.33% to 0.26% at 5.5 ms. The testing results demonstrate that the usage of suggested algorithm can improve infrared imaging quality and radiation measurement accuracy.

PACS numbers: 07.57.Ty

Keywords: Wide dynamic range, Non-uniformity correction, Infrared radiation, Cooling infrared focal plane array

DOI: 10.3938/jkps.73.1821

I. INTRODUCTION

At present, ground-based infrared radiant characteristics measurement (IRCM) systems are widely used by military to track and measure the radiometric characteristics and the space objects in outfield. More specifically, the main purposes and applications for IRCM systems include infrared imaging acquisitions at long distance and infrared radiation characteristics measurement with high precision [1]. Traditional ground-based infrared imaging technology can capture high-signal-to-noise-ratio imaging of aircraft at the distance of tens of kilometers or hundreds of kilometers. However, modern infrared ra-

diation characteristic measurement technology make the radiational acquisition, which includes infrared radiation intensity or infrared radiation temperature [2] of the interested objects quantitatively possible. Above all, both infrared imaging technology and infrared radiation characteristics measurement technology are of great influence in missile penetration, reconnaissance, and evaluation of the stealth performance of weapons. It is an important link in the construction of information equipment system.

However, all the infrared imaging systems equipped with an infrared focal planed array (IRFPA) have the same disadvantage: The fixed pattern noise (FPN) is still the major factor that degrades imaging performance and deteriorates the accuracy of radiant measurement [3]. Analytically, the precise manufactures of the

*E-mail: tianwaishenzhou@163.com

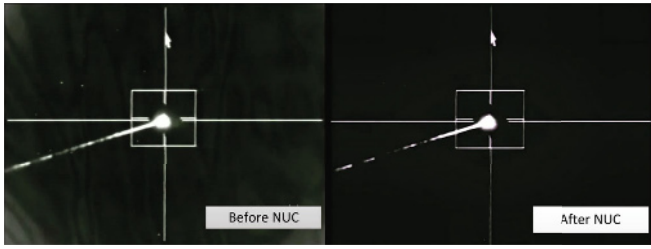


Fig. 1. Effect of the NUC on the image.

IRFPA itself and the optical-mechanical system are the two main factors leading to spatial fixed-pattern noise (FPN), which cause the response for individual pixels to be inconsistent [4,5].

The NUC aims to eliminate the unwanted FPN so that the real infrared data can be obtained to the maximum extent. Currently, typical NUC algorithms are generally classified into two main categories: calibration-based non-uniformity correction (CBNUC) algorithms and scene-based non-uniformity correction (SBNUC) algorithms [6, 7]. The former uses extended surface IR references as uniform temperature sources to determine the suitable correction coefficients [8–10]. The latter is reference-free, and the coefficients for detector signal correction are obtained by using a statistical analysis of the pixel response in real-scene image sequences acquired by using a thermal camera [11,12].

In military, infrared imaging systems are commonly equipped with a cooled IRPFPA as the imaging unit, and the technology for infrared radiation measurements is generally only applicable in the linear response region of IRCM system [14,15]. Therefore, a CBNUC algorithm, especially the typical two point correction, is a linear correction algorithm that is suitable for this type system. The advantages of the algorithm are simple and reliable. Therefore, it is more suitable for determining the NUC for an IRCM system.

In this paper, a wide-dynamic-range NUC algorithm specialized for an IRCM system, which is based on the traditional CBNUC and a model for infrared radiation measurement, is proposed. This algorithm's best advantage is that it fully considers a variable integration time. (We noted that the gray value of a pixel should be neither too low nor too high because a low gray value leads to a poor signal-to-noise ratio while a saturated gray value makes the measurement invalid. Therefore, a floating integration time should be employed according to a different temperature target). This algorithm not only upgrades the accuracy of the infrared radiation measurement but also guarantees the quality of the infrared images at each integration time. The effects before and after the NUC are shown in Fig. 1.

Firstly, the integration-time linear calibration model is used, and the limitations of the traditional NUC algorithm are analyzed in Sec. II. Next, an improved wide-dynamic-range NUC algorithm is proposed in Sec. III.

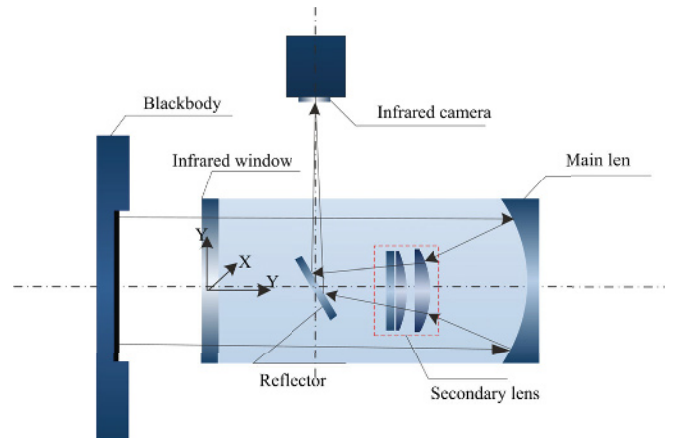


Fig. 2. (Color online) Principle of the radiometric calibration.

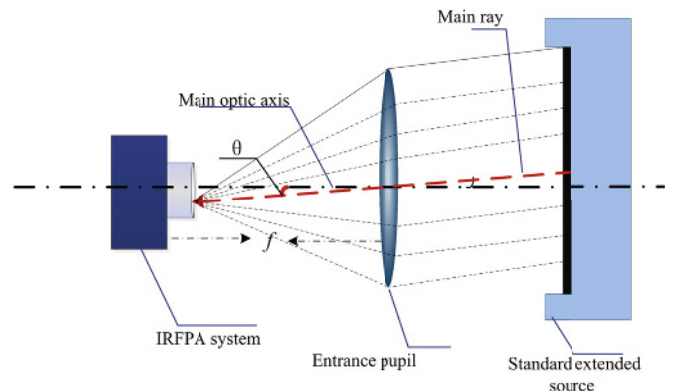


Fig. 3. (Color online) Schematic of single-pixel received energy.

In Sec. IV, a series of radiometric experiments based on a MWIR system with a $\text{\O}400$ mm diameter are carried out in order to verify the described theories. In Sec. V, we present our conclusion that the feasible algorithm not only yields fine quality imaging but also ensures the validity of the infrared radiation data.

II. TRADITION CALIBRATION BASED ON THE NON-UNIFORMITY CORRECTION

1. Integration time linear calibration model

IRCM systems refer to quantitative radiance inversion, so calibration is an indispensable step. Infrared calibration sets up the relationship between the radiance and digital outputs gray value [16–18]. The extended source calibration algorithm is generally adopted in the field in order to eliminate the effects of atmospheric attenuation and atmospheric transmission. The basic principle of the calibration is shown in Fig. 2. A standard reference source is placed near the pupil of the optical system, and

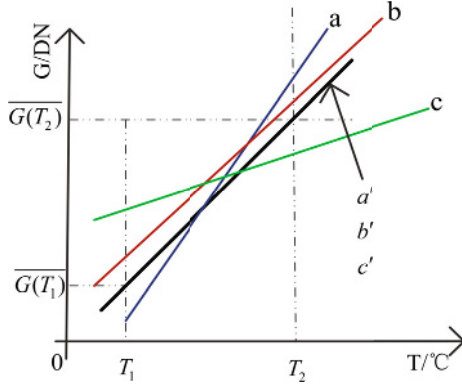


Fig. 4. (Color online) Principle of CBNUC.

the calibration data are obtained by altering the temperature of the standard reference source.

For an IRCM system with a cooled IRFPA, a linear response relationship, which is the basis of infrared radiant characteristics radiometry technology, exist between the gray value and the radiant flux. The relationship between the digital output G (DN) and the radiant flux $\Phi(T)$ (W) for position (i, j) can be described as [19]

$$G_{i,j} = B_{i,j} + R_{i,j} \cdot \Phi(T), \quad (1)$$

where $R_{i,j}$ is the response gain to the radiant flux of the IRCM system, and $B_{i,j}$ is the response offset.

As is shown in Fig. 3, the solid angle $\Omega_{i,j}$ at position (i, j) can normally be given as

$$\Omega_{i,j} = \frac{A_d \cdot \cos \theta_{i,j}}{(f / \cos \theta_{i,j})^2}, \quad (2)$$

where A_d is area of a single pixel and θ is the angle between the main ray and the main optic axis. The radiant flux $\Phi(T)$ in a pixel with A_d can be expressed as

$$\begin{aligned} \Phi(T) &= \tau_{\text{opt}} \cdot L(T) \cdot \left(\frac{\pi}{4} \cdot D^2 \cdot \cos \theta_{i,j} \right) \cdot \Omega_{i,j} \\ &= R \cdot L(T), \end{aligned} \quad (3)$$

where τ_{opt} is the transmittance of the infrared optic system. Supposed that the parameter R is set as

$$R = \frac{\pi}{4} \cdot \tau_{\text{opt}} \cdot \cos^4 \theta_{i,j} \cdot A_d \cdot \frac{D^2}{f^2}, \quad (4)$$

We can see that the parameters are unrelated with radiance $L(T)$, so we can obtain

$$G_{i,j} = B_{i,j} + R_{i,j} \cdot L(T), \quad (5)$$

According to Planck's blackbody raditim theory, the relationship between the gray value G and the radiance $L(T)$ is as follows:

$$G = t \cdot R_{i,j} \cdot L(T), \quad (6)$$

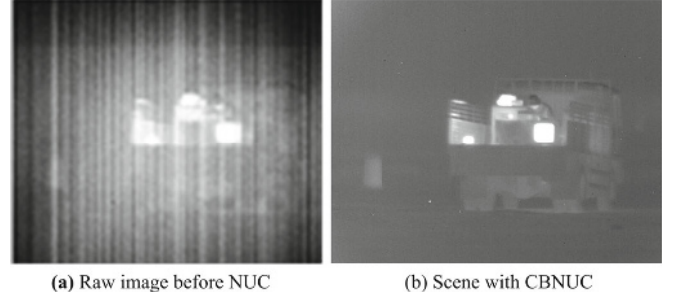


Fig. 5. Result with the CBNUC.

The offset $B_{i,j}$ can be broadly classified into two categories: one (B_{out}) is related to the integration time, and the other (B_{in}) is independent of he integration time. Thus, the offset $B_{i,j}$ can be described as

$$B_{i,j} = B_{\text{out},i,j} + B_{\text{in},i,j}, \quad (7)$$

According to Eqs. (5), (6), and (7), the considered integration time linear calibration model can be described by using

$$G_{i,j}(t, T) = t \cdot R_{i,j} \cdot L(T) + t \cdot B_{\text{out},i,j} + B_{\text{in},i,j}, \quad (8)$$

The above formula reflects the relationship of the gray value G to the object's radiance $L(T)$ and the integration time t . The parameter t is introduced to increase the dynamic range of the IRCM system.

2. CBNUC algorithm

The CBNUC algorithm is one of the most common NUC algorithms for ground-based IRCMS system. Specifically, a standard extended calibration source (black body) is used to acquire images of standard extended sources at different temperatures at a fixed integration time. In another way, a series of images are taken at several integration times at a fixed temperature.

Ideally, for an IRCM system, two images with different temperatures can be collected and used for the non-uniformity correction ideally [20–22]. In fact, several images are usually selected to calculate the average in order to reduce the impact of random errors.

Assuming that the integration time is t_0 and the temperatures are T_1 and T_2 ($T_1 < T_2$), according to the above calibration model, we get:

$$\begin{cases} G(T_1) = t_0 \cdot R \cdot L(T_1) + t_0 \cdot B_{\text{out}} + B_{\text{in}} \\ G(T_2) = t_0 \cdot R \cdot L(T_2) + t_0 \cdot B_{\text{out}} + B_{\text{in}}. \end{cases} \quad (9)$$

The number of pixels of IRFPA is $M \times N$ and the images are collected at temperature T . The average $\overline{G}(T)$ of the IRFPA can be described by using

$$\overline{G}(T) = \frac{\sum_{i=1}^M \sum_{j=1}^N G(T)}{M \times N}. \quad (10)$$

Table 1. Parameters of the IRCM system.

F/#	2
Focal length	800 mm
Band	3.7 ~ 4.8 μm
Pixel size	30 $\mu\text{m} \times 30 \mu\text{m}$
Number of pixels	320 \times 256

Table 2. Standard extended source parameters.

Type name	SR800 by CI company
Emitting area	500 mm \times 500 mm
Temperature accuracy	± 0.1 $^{\circ}\text{C}$
Emissivity	0.97 ± 0.03
Temperature range	5 ~ 150 $^{\circ}\text{C}$

The basic principle of CBNUC algorithm is shown in Fig. 4. In the figure, the letters a , b , and c are the response curves before the NUC and a' , b' , c' are the response curves after the NUC. We can see the response curves tend to be consistent. The CBNUC correction coefficients can be expressed as

$$\begin{cases} k^{(t_0)} = \frac{\overline{G(T_2)} - \overline{G(T_1)}}{G(T_2) - G(T_1)} \\ b^{(t_0)} = \overline{G(T_2)} - k^{(t_0)} \cdot G(T_2). \end{cases} \quad (11)$$

The usage of CBNUC correction coefficients can improve the the quality of MWIR images at integration time t_0 . The results are shown in the Fig. 5.

III. WIDE-DYNAMIC-RANGE NUC ALGORITHM

Different from a traditional infrared imaging system, IRCM systems not only provide a series of high-quality images but also ensure the validity of radiometric data in outfield. However, traditional NUC coefficients, which are limited by the variable integration time, will bring about a great number of images with low signal-to-noise ratios. In order to adapt the NUC to a wide-dynamic-range IRCM system in the field, in this paper, we propose a wide dynamic range NUC algorithm.

A raw image $G_{i,j}(t, T)$ is obtained by using the CBNUC $k_{i,j}^t(T)$, $b_{i,j}^t(T)$, and the corrected result $G_{i,j}^{(c)}(t, T)$ can be described using

$$\begin{aligned} G_{i,j}^{(c)}(t, T) &= k_{i,j}^t(T) \cdot G_{i,j}(t, T) + b_{i,j}^t(T) \\ &= \overline{G_{i,j}(t, T)}. \end{aligned} \quad (12)$$

According to the CBNUC algorithm, at integration times t_1 and t_2 , and temperatures T_1 and T_2 , we get

$$k_{i,j}^t(T) = k_{i,j}^{t_1}(T), \quad (13)$$

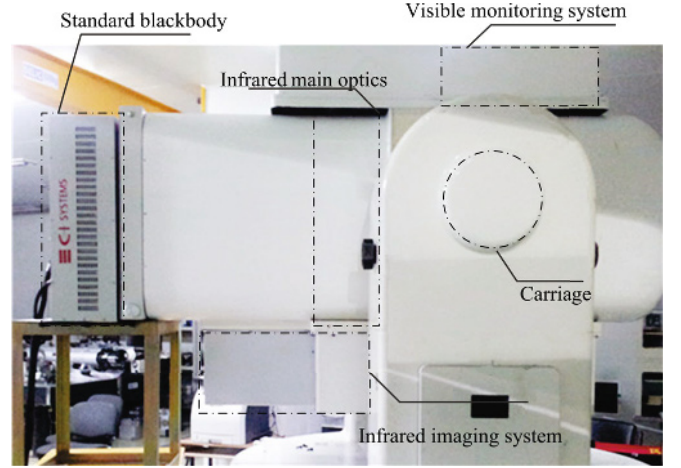


Fig. 6. (Color online) Calibration and NUC setup.

$$t_1 \cdot \overline{B_{\text{out}}} + \overline{B_{\text{in}}} = k_{i,j}^{t_1}(T) \cdot (t_1 \cdot B_{\text{out},i,j} + B_{\text{in},i,j}) + b_{i,j}^{t_1}(T), \quad (14)$$

In the same way,

$$t_2 \cdot \overline{B_{\text{out}}} + \overline{B_{\text{in}}} = k_{i,j}^{t_2}(T) \cdot (t_2 \cdot B_{\text{out},i,j} + B_{\text{in},i,j}) + b_{i,j}^{t_2}(T), \quad (15)$$

$$t \cdot \overline{B_{\text{out}}} + \overline{B_{\text{in}}} = k_{i,j}^t(T) \cdot (t \cdot B_{\text{out},i,j} + B_{\text{in},i,j}) + b_{i,j}^t(T), \quad (16)$$

Combined with Eqs. (14), (15), and (16):

$$b_{i,j}^t(T) = \frac{t - t_1}{t_2 - t_1} \cdot b_{i,j}^{t_2}(T) - \frac{t - t_2}{t_2 - t_1} \cdot b_{i,j}^{t_1}(T), \quad (17)$$

Finally,

$$\begin{cases} K_{i,j}^t(T) = K_{i,j}^{t_1}(T) \\ B_{i,j}^t(T) = \frac{t - t_1}{t_2 - t_1} \cdot B_{i,j}^{t_2}(T) - \frac{t - t_2}{t_2 - t_1} \cdot B_{i,j}^{t_1}(T). \end{cases} \quad (18)$$

IV. EXPERIMENT

To verify the wide-dynamic-range NUC algorithm proposed in this paper, we performed a series of experiments by using a 400 mm mid-wave IRCM system. The system's parameters are given in Table 1, and the standard extended source parameters are given in Table 2.

The calibration device and the infrared radiometry system are shown in Fig. 6. As we all know, the considered integration time linear calibration model is the basis for infrared radiant characteristics radiometry technology and the wide-dynamic-range NUC algorithm for verifying the relationship between the gray value G and the radiance $L(T)$, as well as the integration time t .

In this experiment, integration times of 2.5 ms, 4 ms and 5.5 ms are employed in the IRCM system. The parameters of the IRCM system are given in. The range of the standard extended source's temperature is varied from 30 ~ 90 $^{\circ}\text{C}$ in intervals of 5 $^{\circ}\text{C}$. Finally, the fitting

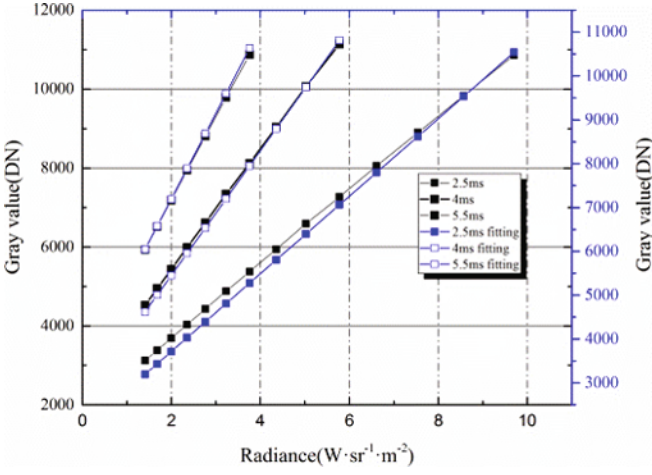


Fig. 7. (Color online) Relationship between the gray value and the radiance.

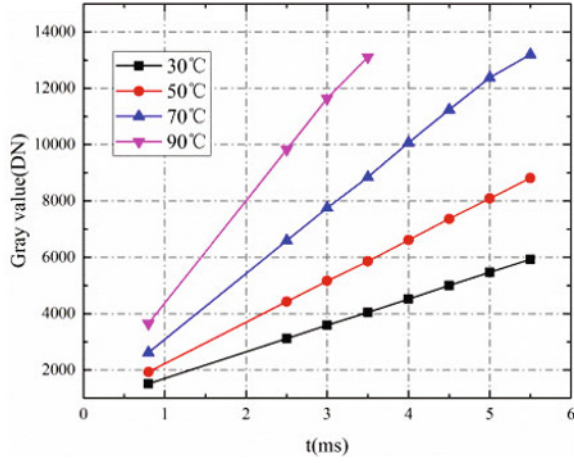


Fig. 8. (Color online) Relationship between the gray value and the integration time at various temperatures.

curve for the gray value G vs. the radiance $L(T)$ is displayed in Fig. 7. At fixed temperatures of 30 °C, 50 °C, 70 °C, and 90 °C, the integration time is changed from 0.5 ms to 5.5 ms in 0.5 ms steps. The data relating the gray value G to the integration time were fitted, and the result is shown in Fig. 8. One can see that good linear relationships between the gray value and the radiance, and the integration time are achieved as expected.

In order to evaluate the non-uniformity of the IRPFA, we adopted a typical evaluation function [23]:

$$\begin{cases} NU = \frac{1}{\bar{G}} \times \sqrt{\frac{1}{M \times N - d} \cdot \sum_{i=1}^M \sum_{j=1}^N (G_{i,j} - \bar{G})^2} \times 100\% \\ \bar{G} = \frac{1}{M \times N - d} \cdot \sum_{i=1}^M \sum_{j=1}^N G_{i,j}, \end{cases} \quad (19)$$

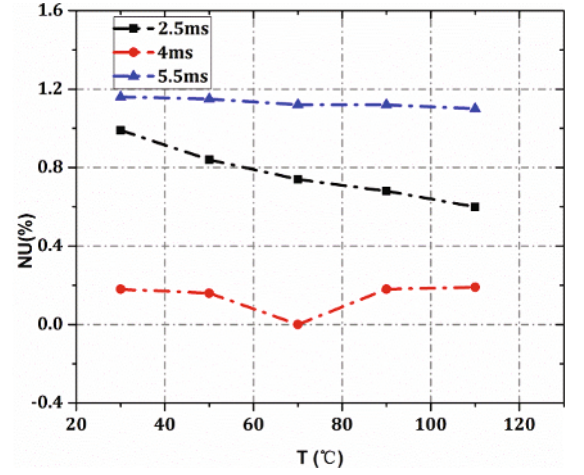


Fig. 9. (Color online) Variation of the non-uniformity with temperature for these integration time.

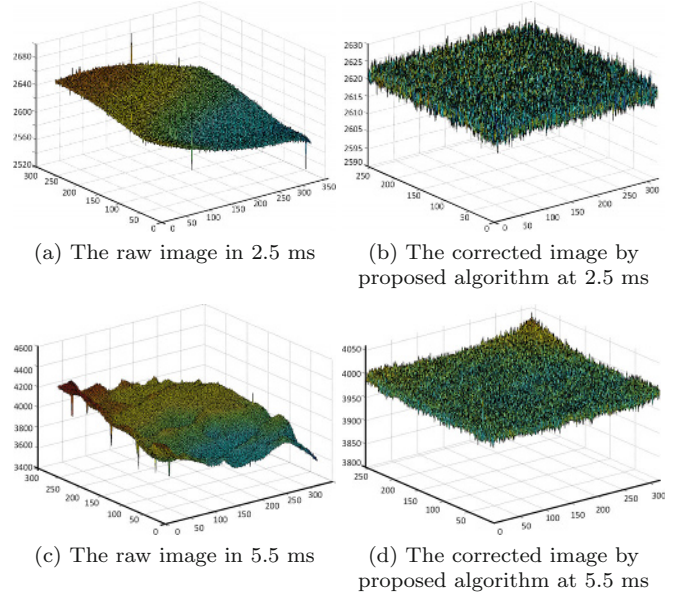
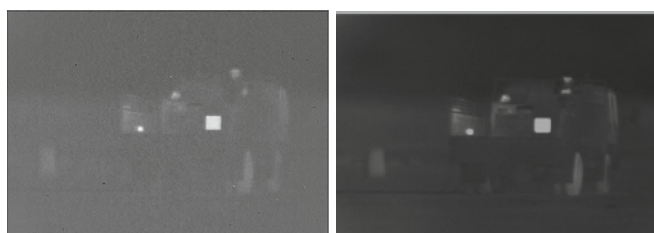


Fig. 10. (Color online) Images before and after the application of the NUC.

where d is the number of bad pixels. For temperatures 60 °C and 70 °C and an integration time of 4 ms, the coefficients from the CBNUC algorithm can be calculated. The 4 ms images were corrected, and the average non-uniformity was 0.23% for temperatures of 30 °C, 50 °C, 70 °C, 90 °C and 110. However, at those temperatures, the average non-uniformity deteriorated to 0.77% at 2.5 ms and 1.33% at 5.5 ms. The variation of the non-uniformity degree with temperature is shown in Fig. 9. One can see that the corrected results for other integration times will be worse than those for an integration time of 4 ms.

For comparing the traditional CBNUC algorithm, images at 2.5 ms and 5.5 ms were obtained simultaneously using the wide-dynamic-range NUC algorithm; the aver-



(a)The scene at 2.5 ms

(b)The scene at 5.5 ms

Fig. 11. Images corrected by using the proposed algorithm at integration time of (a) 2.5 ms and (b) 5.5 ms.

age degrees of non-uniformity at two times were 0.21% and 0.26% respectively. One can see that the better non-uniformity degree was achieved by using the proposed algorithm with different integration times. The trends of gray value trendy are displayed in Fig. 10. Figures 10(a) and (c) show the raw image for integration time of 2.5 and 5.5 ms respectively, and Figs. 10(b) and (d) show images that were obtained after applying the NUC with the proposed algorithms. Finally, the real scene raw images acquired at 2.5 ms and 5.5 ms were corrected using wide-dynamic-range NUC algorithm, and the resulting images were shown in Figs. 11(a) and (b), respectively.

V. CONCLUSION

In this paper, based on the integration time linear calibration model, we analyzed the limitations of traditional CBNUC algorithm applied to an IRCM system. Considering approaching demands and the uncertainty in the infrared radiant characteristics measurement in outfield, we propose a wide-dynamic-range NUC algorithm suited for IRCM system. This algorithm satisfies the special requirements that IRCM systems not only provide-high-quality images but also ensure the validity of the infrared measurement data. Compared with traditional CBNUC technology, the technology required for the NUC process and equipment is simpler and the workload and compu-

tational complexity is greatly reduced. To sum up, the real-time performance of an IRCM system is improved when the proposed algorithm is used.

REFERENCES

- [1] S. E. Godoy *et al.*, *Applied Optics* **47**, 5894 (2008).
- [2] U. Sakoglu *et al.*, *Proc. SPIE* **5558**, 69 (2004).
- [3] Gutschwager *et al.*, *Appl. Opt.* **54**, 10599 (2015).
- [4] V. F. Paz *et al.*, *Light Science & Applications* **1**, e36 (2012).
- [5] A. F. Milton *et al.*, *Optical Engineering* **24**, 855 (1985).
- [6] Y. Cao *et al.*, *Applied Optics* **52**, 6266 (2013).
- [7] D. R. Pipa *et al.*, *IEEE Transactions on Image Processing* A Publication of the IEEE Signal Processing Society **21**, 4758 (2012).
- [8] E. Vera *et al.*, *Optics Letters* **36**, 352 (2011).
- [9] M. J. Booth *et al.*, *Light Science & Applications* **3**, e165 (2014).
- [10] C. Zuo *et al.* *Optik - International Journal for Light and Electron Optics* **123**, 833 (2012).
- [11] Jin *et al.* *Infrared Physics & Technology* **78**, 1 (2016).
- [12] M. Yan *et al.*, *Light Science & Applications*, **6**, e17076 (2016).
- [13] N. Meitav *et al.* *Light Science & Applications*, **5**, e16048 (2016).
- [14] Sheng-Hui *et al.*, *J. Opt. Soc. Am. A Opt. Image Sci. Vis.* **33**, 938 (2016).
- [15] C. Zuo *et al.*, *Optical Review* **18**, 197 (2011).
- [16] M. Ochs *et al.*, *Infrared Physics & Technology*, **53**, 112 (2010).
- [17] J. Zhang *et al.*, *Light Science & Applications* **7**, 17180 (2018).
- [18] W. W. Hauswirth *et al.*, *Journal of Vision* **9**, 27 (2009).
- [19] Z. Liu *et al.*, *Infrared Physics & Technology* **76**, 667 (2016).
- [20] W. Qian *et al.*, *Applied Optics*, **50**, 1 (2011).
- [21] C. C. Hou *et al.*, *Light Science & Applications* **7**, 17170 (2018).
- [22] J. Zhao *et al.*, *Optics Communications* **296**, 47 (2013).
- [23] H. X Zhou *et al.*, *Infrared Physics & Technology* **53**, 295 (2010).